

A Single-bounce Channel Model for Dense Urban Street Microcell

Mir Ghoraishi Jun-ichi Takada
 Department of International Development Engineering
 Tokyo Institute of Technology
 Tokyo, 152-8550, Japan
 {mir, takada}@ap.ide.titech.ac.jp

Tetsuro Imai
 R&D Center
 NTT DoCoMo Inc.
 Kanagawa, 239-8536, Japan
 imai@mlab.yrp.nttdocomo.co.jp

ABSTRACT

A channel model for line-of-sight (LoS) small street microcell in dense urban areas is proposed. The distribution of the scatterers in the channel seen from the receiver (Rx) based on the physical phenomenon is obtained. The coefficients of the distribution function is derived by approximation to a set of urban street microcell measurement data. The power-azimuth spectrum (PAS) for the proposed model is compared with those for conventional elliptical model as well as with experimental results obtained from measurement in streets with three different widths. It is shown that the proposed model in contrast to the conventional models produces results that closely agrees with the experimental results.

I. INTRODUCTION

Characterization and modeling of the radio propagation channel are essential for mobile and wireless systems design. A detailed knowledge about mobile communication propagation channel leads to a more successful design of the communication system. Especially to design and evaluate the multi-antenna systems understanding the spatial properties of the channel is a prerequisite. An overview of the existing spatial channel models is available at [1]. One of the most commonly used directional channel models is based on a geometric description of the scattering process, which focuses on the detailed internal construction or realization of the channel. The model assumes a statistical distribution of scatterers in the wireless link and channel properties are derived from the positions of the scatterers by applying the fundamental laws of propagation mechanism of electromagnetic waves. Single-bounce scattering geometric models are among the most widely used geometric models, where propagation between the transmitter (Tx) and receiver (Rx) antennas is assumed to take place via single scattering from an intervening obstacle. Usually the bistatic scattering cross section of the scatterer is assumed to be isotropic, but its density is assumed to vary from location to location. Geometrical modeling of the propagation channel has always been attractive for the researchers due to its advantages. The very well known Jakes model is a geometrical channel model itself [3]. In this model the scatterers are considered to be uniformly distributed over a circular ring. The model proposed in [4] is circular as well however the scatterers are assumed to be uniformly distributed within a circular disk

while [5] proposes a circular gaussian scattering distribution of scatterers around mobile station. In the models suggested in [6], [7] the scatterers are considered to be distributed over an elliptical disk. The major axis of the ellipse is assumed to be along the base station to mobile axis in [6] while in [7] it has aligned to the street where mobile is located. All of these models only the local scattering cluster which is located around the mobile station is taken into account. Therefore these models are suitable for macrocell environments where base station antenna heights are relatively large and therefore there is no signal scattering from locations near the base station. As a result, for scenarios where scatterers are located around base station as well as mobile station the model's performance degrades.

For the small cells with relatively low height antennas the elliptical model called geometrically based single bounce elliptical model (GBSBEM) proposed in [1], [8] is more attractive. The model assumes a uniform distribution of the scatterers within an ellipse where the base station and mobile are the foci of the ellipse and therefore scattering near the base station is as likely as near the mobile. Nonuniform distribution of the scatterers over the ellipse was suggested in [9] by dividing the main ellipse into a number of elliptical subregions where each subregion correspond to one range of excess delay time. The number of scatterers within each subregion is selected from a Poisson random variable with its mean chosen from the measured power delay spectrum. The elliptical models are particularly attractive for consideration of the locus of the scatterers with the same delay. They have been widely used in the literature and simulation of the microcell and even macrocell (e.g. in [10]).

Geometric channel models are well suited for simulations. The advantage of these models is their simplicity for simulation. The shape and size of the spatial scatterer density function required to achieve a reliable simulation of the propagation phenomenon however is subject to debate [11]. The main drawback of the geometric channel models is that only a single specular reflection is accounted for and neither scattering, diffraction, nor multiple bounces are considered.

In particular, for a street microcell, the single-bounce assumption is rather restrictive as by no means the street width is sufficient to match the ellipse of the maximum delay. To overcome this shortage the concept of *effective street width* was introduced in [12]. In a street microcell scenario, the base

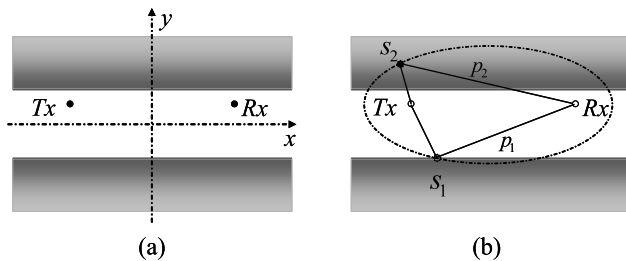


Fig. 1. (a) The street microcell scenario and the definition of axes. (b) An ellipse with Tx and Rx locations as its foci.

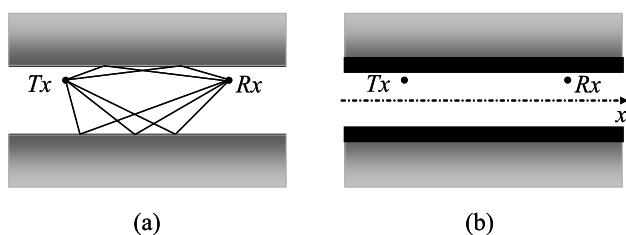


Fig. 2. (a) A few uni-reflection paths. (b) The locus of the uni-reflection path scattering points.

station and the mobile are not so far from each other. Moreover the antenna heights are lower than the surrounding buildings. In such a scenario the propagation channel is experiencing severe multireflections. Considering the locus of the scatterers with equal delays, as it is in the elliptical models, is not sufficient. In fact, the prime importance in a propagation channel is the scattering loss or path gain.

In this paper we introduce a scattering distribution function based on major propagation mechanisms in the street microcell. In the proposed model the multi-reflections are taken into account however we visualize them as single-bounce scatterers. By this we can give the distribution of the scatterers to develop the model, however this is not according to the definition of the geometrical modeling. Hence we call this model a pseudo-geometrical channel model. The physical description of the model is described in section II and the scattering distribution is obtained in III. In section IV the coefficients for the proposed model is given using measurement data. The power-azimuth spectrum (PAS) from the proposed model is compared to PAS of GSBEM and the measurement data in section V. Section VI is conclusion.

II. MODEL DESCRIPTION

The presumptions for the model are as following:

- Tx and Rx are in the same street, that is the scenario is line-of-sight (LoS).
- Channel is two dimensional that is Tx, Rx and the scatterers are in the same plane. This is a regular assumption for most geometrical models.
- Tx and Rx antenna heights are lower than surrounding buildings.
- A street surrounded by dense tall buildings with no building irregularity is assumed. No crossing road and

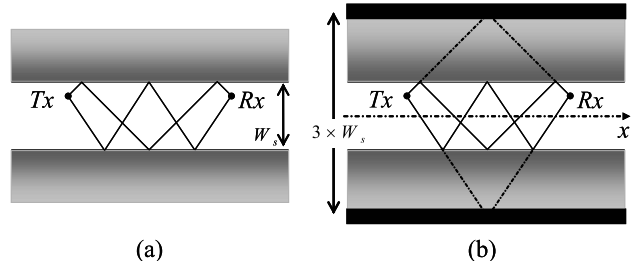


Fig. 3. (a) Two tri-reflection paths. (b) The locus of the tri-reflection paths single-bounce scattering points.

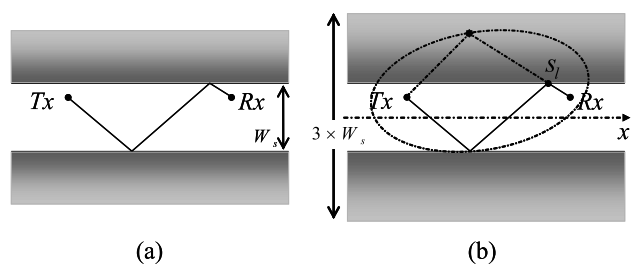


Fig. 4. (a) A bi-reflection path. (b) The equivalent single-bounce scattering point.

no additional object in the environment is considered.

The schematic of such a scenario is shown in Fig.1. For clarity an ellipse according to the conventional model has been sketched as well. Obviously the scattering point s_2 can not be inside the building zone and path p_2 might be a multi-reflected wave, however to make the analysis simpler and to obtain a pseudo-geometrical distribution for the scatterers we present the scatterers as single-bounce. By this assumption, the scattering point for path p_2 is identified at s_2 located on the cross point of the ellipse with the path length equal to p_2 and the radial line from the Rx with an azimuth equal to the azimuth-of-arrival (AoA) of p_2 . Next we observe that even though both s_1 and s_2 make equal-length paths and therefore equal free space path losses, the actual path losses can be very different. This is because p_1 is a multi-reflected path but s_1 is not. In fact, in small scenarios due to the small distance between base station and the mobile, the dominant paths are not so long. On the other hand because of smaller height of the both link ends antennas the channel is experiencing severe multi-scatterings. That is the scattering loss for each path is large. Therefore the dominant loss in these scenarios is scattering loss.

Consequently the ellipse with Tx and Rx as its foci may not be a good choice for the geometrical locus of the scatterers. Instead, we are after the locus of the scattering points for the paths with equal number of reflections. Fig. 2(a) illustrates a few uni-reflection received paths and Fig. 2(b) is the locus of these scatterers. The locus of these scatterers are two bands along two sidewalls of the street. It has to be noted that the symmetry axis for the distribution of these points is not the Tx-Rx axes but the x axis. On the other hand, Fig. 3(a)

shows two tri-reflection paths, and in Fig. 3(b) the locus of the single-bounce equivalent scattering points of these paths has been illustrated. It indicates that the locus is two bands of $3W_s$ apart parallel to the street walls. It is also clear that the symmetry axis for the locus is again the x axis. A similar description can be given for all odd-number-reflection paths and it can be observed that the axes of symmetry is always x axis.

Figure 4 illustrates a bi-reflection path. Obviously the single-bounce scattering point for this path lies somewhere between uni- and tri-reflection path scattering point locus. The single-bounce scattering point for bi-reflection path can be obtained by first identifying s_l the last scattering point of the path using its AoA and then drawing the ellipse with foci of Tx and s_l and the major axes of the path length up to the s_l . The single-bounce scattering point will then be obtained using this ellipse and the AoA.

The previously described geometrical locus of the scatterers indicates that the scattering loss is linearly increasing along the y axis in both directions. This is because as the scattering point is considered deeper into the building zone the path has experienced a larger number of scatterings. On the other hand, there is no scatterings inside the street in ideal case as it is assumed that there is no scatterer. In practice however, scatterings happens due to existence of the objects in this area. Therefore we expect to have similar trend but in a lower rate in the street as well. That is the scattering loss increases along the x axis as scatterer moves further from Tx or Rx.

III. SCATTERING DISTRIBUTION

The experimental results from measurements in the dense urban street microcell shows that the scattering distribution has an elliptical shape but is different from conventional ellipse because most scatterers are distributed along the street. This agrees with the description presented in section II which indicates that the scattering distribution diminishes more rapidly along the y axis compared to those along x axis. An ellipse with a focus larger than the focus of the conventional ellipse is proposed here as the shape of the scatterer distribution. The foci of this ellipse are on the x axes. The scattering distribution in the street P_s and inside the building zones P_b are defined as following and shown in Fig. 5:

$$P_s = e^{-\left\{\sqrt{\alpha_x(x-f_n)^2} + \sqrt{\alpha_x(x+f_n)^2} + C_x\right\}}$$

$$P_b = e^{-\left\{\sqrt{\alpha_y y^2 + \alpha_x(x-f_n)^2} + \sqrt{\alpha_y y^2 + \alpha_x(x+f_n)^2} + C_y\right\}}$$

where f_n is the focus parameter, α_x and α_y are loss coefficients along x and y axes respectively and C_x and C_y are constants.

IV. DISTRIBUTION COEFFICIENTS

In this section the results from a set of measurements in the dense urban areas are used to obtain the parameters of the scattering distribution. The measurement has been accomplished for a small microcell LoS scenario [13]. Both the Tx and Rx antennas were installed at equal height of 3 meters from the ground level. The measurements were performed in 3 streets

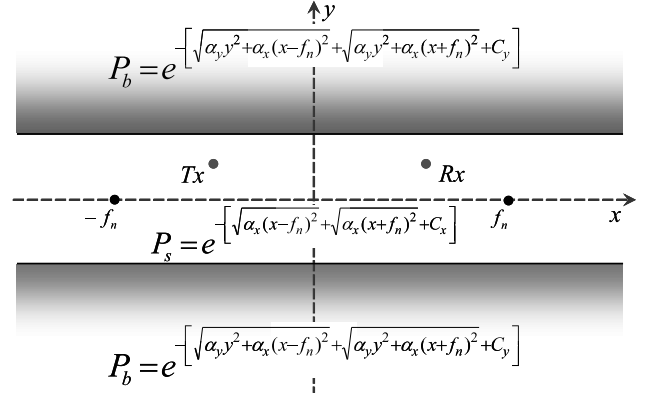


Fig. 5. The distribution function of the scatterers.

with different widths of 26, 18 and 10 m. The received data was recorded for two different position of Rx in the street of 26 m wide and for 3 different positions in each of the other streets. The Tx to Rx distance was always 60 m fixed. The average height of the surrounding buildings is 30 m. The details of the measurement campaign is explained in [13]. The coefficients for the scattering distribution for each environment can be acquired from the directional measurement data. Fig. 6 shows the measured received power along x axis. In this figure the Tx position for both measurement data is at 100 m and of Rx on 160 m. The solid line in this figure is the following approximation:

$$L = L_0 + \alpha_L(l_p - l_{LoS}) + \beta_L$$

In this equation L is the path loss, L_0 is the free space path loss, l_p is the path length, l_{LoS} is the LoS distance and α_L and β_L are constants related to α_x and C_x . A similar process is performed for the y axis. Fig. 7 shows the measured received power for the point on the y axis and the solid line is the approximation:

$$L = L_0 + \alpha_W(l_p - l_{LoS}) + \beta_W$$

where α_W and β_W are constants related to α_y and C_y . With simple mathematical techniques the values of α_x , α_y , C_x , C_y and f_n can be obtained from these approximations.

V. POWER AZIMUTH SPECTRUM

To evaluate the goodness of the proposed scattering distribution a directional parameter of the model shall be compared to the experimental results. For this purpose, the PAS acquired from measurement data for each of the streets was compared to the one calculated from proposed scatterer distribution. Fig. 8 illustrates this for the street of 26 m wide. For comparison the PAS obtained from GBSBEM model is included as well. The azimuth of 0° is the Tx direction and increases clockwise. The LoS component is not included in the models, therefore at the azimuth values around 0° and 360° the measurement data and the PAS obtained from models are different. For the non-LoS components, the proposed model obviously matches better than the conventional elliptical model with the measurement

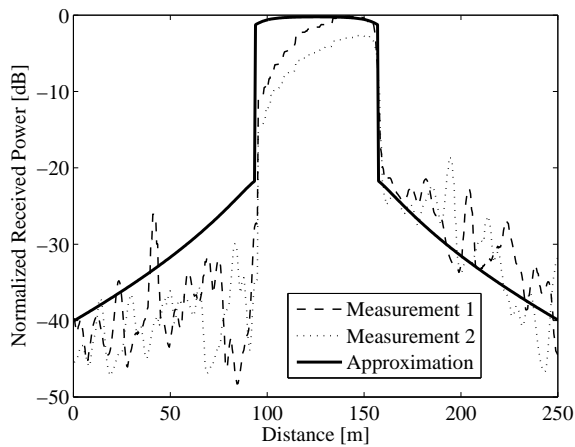


Fig. 6. The measured received power along x axis and the approximation, street width=26 m.

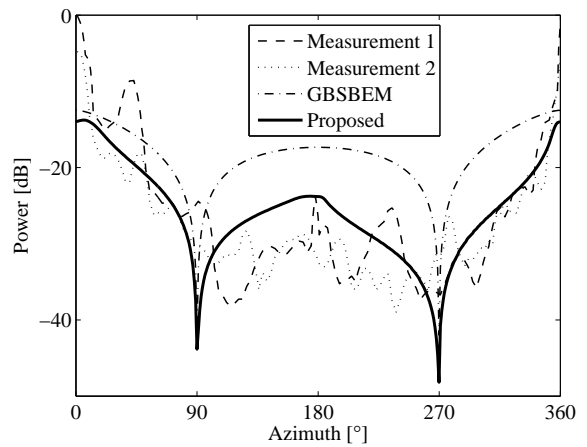


Fig. 8. The PAS from measurements, GBSBEM and proposed model, street width=26 m.

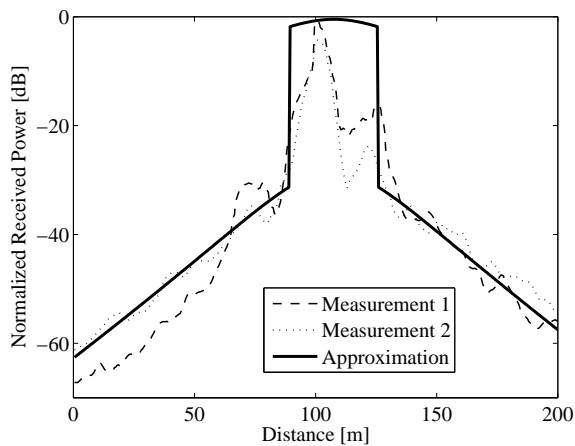


Fig. 7. The measured received power along y axis and the approximation, street width=26 m.

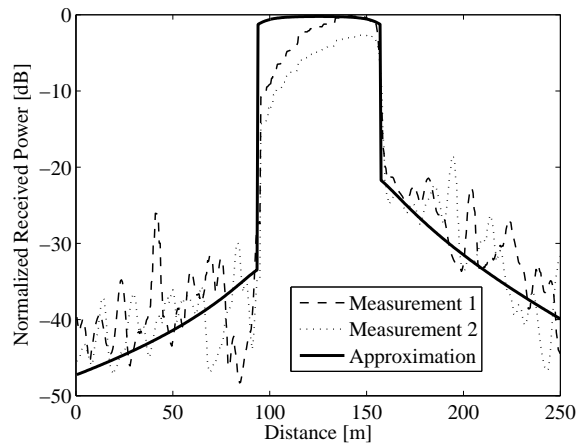


Fig. 9. The measured received power along x axis and the modified approximation, street width=26 m.

data. For the azimuth values less than 90° and more than 270° the proposed model's PAS matches well to the measurement data. However on the azimuth values between 90° and 270° that is for the minus values of x the performance of the proposed model shows minor degradation. The same trend was observed for the other two streets as well. The reason is investigated by a precise look at the Fig. 6. It can be observed that for the distances less than 100 m that is close to Tx but on the opposite side of the Rx, the linear approximation does not match precisely to the measurement data. This is most likely the effect of a crossing street at this locations, however to confirm the reason for this phenomenon measurements in more streets are necessary. To improve the model different coefficients for the negative and positive parts of the x axis were estimated. The result is shown in Fig. 9. The PAS of the proposed model after this modification is illustrated in Fig. 10 and the improvement is clear.

Same process was performed for other two streets and the PAS

obtained from two models and from experiments are shown in Fig. 11 and Fig. 11. The PAS obtained from the model after modification is obviously matching the measurement results better than conventional elliptical model. Table I shows the values for three streets. It is observed that the coefficients for the scattering distribution are dependent on the street width. The dependency of the coefficients to other parameters like antenna height, base station to mobile distance, surrounding building height, etc. could not be analyzed due to lack of appropriate measurement data.

VI. SUMMARY

A channel model according to the physical mechanisms in the street microcell was proposed. The expression for the scattering distribution was provided and the necessary parameters for the distribution estimated from the measurements data. The PAS predicted by the model were compared to those of conventional elliptical model and experimental results. The

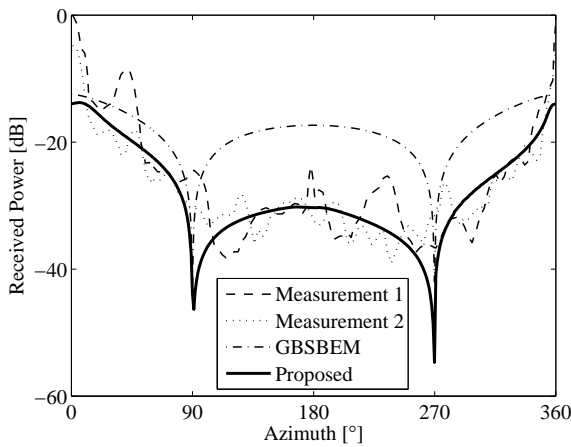


Fig. 10. The PAS from measurements, GBSBEM and modified model, street width=26 m.

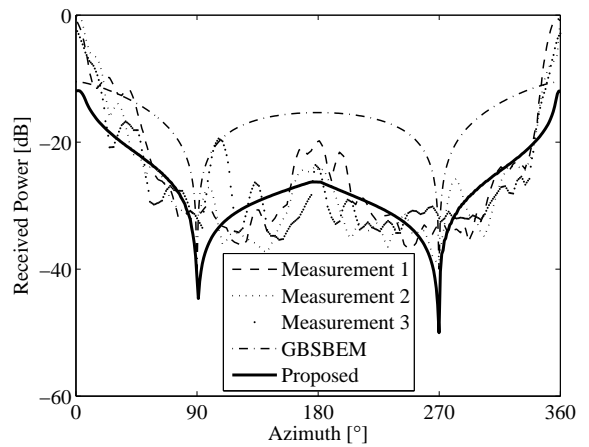


Fig. 12. The PAS from measurements, GBSBEM and modified model, street width=10 m.

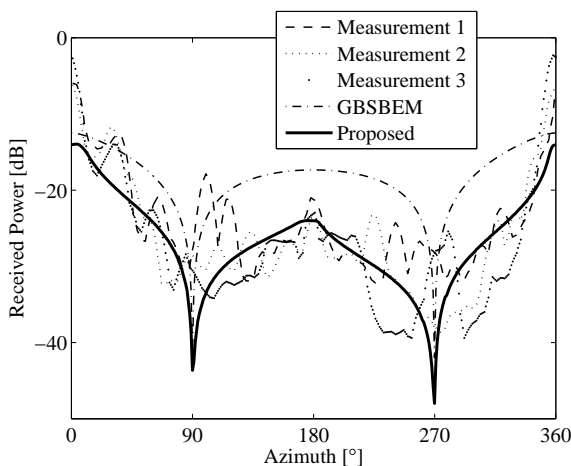


Fig. 11. The PAS from measurements, GBSBEM and modified model, street width=18 m.

PAS of the proposed model matches to the experimental results better than the conventional models.

REFERENCES

[1] R. Ertel, P. Cardieri, K. Sowerby, T. Rappaport, J. Reed, "Overview of spatial channel models for antenna array communication systems," *IEEE Personal Communication Magazine*, Vol. 5, No. 1, pp. 10-22, Feb. 1998.

[2] U. Martin, J. Fuhl, I. Gaspard, M. Haardt, A. Kuchar, C. Math, A. Molisch, R. Thoma, "Model Scenarios for Direction-Selective Adaptive Antennas in Cellular Mobile Communication Systems Scanning the Literature," *Wireless Personal Communications*, Vol. 11, No. 1, pp. 109-129, Oct. 1999.

[3] W. Jakes, *Microwave Mobile Communications*, IEEE Press, 1974.

[4] P. Petrus, J. Reed, T. Rappaport, "Geometrical-Based Statistical Macrocell Channel Model for Mobile Environments," *IEEE Transactions on Communications*, Vol.50, No.3, pp. 495-502, March 2002.

[5] R. Janaswamy, "Angle and time of arrival statistics for the Gaussian scatter density model," *IEEE Transactions on Wireless Communications*, Vol. 1, No. 3, pp. 488-497, July 2002.

TABLE I
LOSS COEFFICIENTS

Street Width [m]	α_x	α_y
26	1.0×10^{-3}	1.0×10^{-4}
18	2.1×10^{-3}	2.0×10^{-4}
10	3.0×10^{-3}	2.6×10^{-4}

[6] T. Fujii, H. Omote, "Time-spatial path modeling for wideband mobile propagation," *Proceedings of the IEEE Vehicular Technology Conference (VTC'04 Fall)*, Vol. 1, pp. 120-124, Sep. 2004.

[7] T. Imai, T. Taga, "Stochastic model of scattering component distribution in outdoor propagation environment," *Proceedings of the IEEE Vehicular Technology Conference (VTC'03 Fall)*, Vol. 1, pp. 104-108, Oct. 2003.

[8] J. Liberti, T. Rappaport, "A geometrically based model for line-of-sight multipath radio channels," *Proceedings of the IEEE Vehicular Technology Conference (VTC'96)*, Vol.2, pp. 844-848, May 1996.

[9] M. Lu, T. Lo, J. Litva, "A physical spatio-temporal model of multipath propagation channels," *Proceedings of the IEEE Vehicular Technology Conference (VTC'97)*, Vol. 2, pp. 810-814, May 1997.

[10] C. Oestges, V. Erceg, A. Paulraj, "A physical scattering model for MIMO macrocellular broadband wireless channels," *IEEE Journal on Selected Areas in Communications*, Vol. 21, No. 5, pp. 721-729, June 2003.

[11] Y. Chen, V. Dubey, "Accuracy of geometric channel-modeling methods," *IEEE Transactions on Vehicular Technology*, Vol.53, No.1, pp. 82-93, Jan. 2004.

[12] M. Marques, L. Correia, "A wideband directional channel model for UMTS microcells," *Proceedings of the IEEE International Symposium on Personal, Indoor and Mobile Radio Communications (PIMRC'01)*, Vol. 1, pp. B-122-B-126, Sept. 2001.

[13] M. Ghoraiishi, J. Takada and T. Imai, "Microcell Urban Propagation Channel Analysis Using Measurement Data," *Proceedings of the IEEE Vehicular Technology Conference (VTC'05 Fall)*, Vol. 3, pp. 1728-1731, Sept. 2005.